

# Low loss hollow-core waveguide on a silicon substrate

Weijian Yang<sup>1</sup>, James Ferrara<sup>1</sup>, Karen Grutter<sup>1</sup>,  
Anthony Yeh<sup>1</sup>, Chris Chase<sup>1</sup>, Yang Yue<sup>2</sup>,  
Alan E. Willner<sup>2</sup>, Ming C. Wu<sup>1</sup>  
and Connie J. Chang-Hasnain<sup>1,\*</sup>

<sup>1</sup>Department of Electrical Engineering and Computer Sciences, University of California at Berkeley, Berkeley, CA 94720, USA

<sup>2</sup>Department of Electrical Engineering, University of Southern California, Los Angeles, CA 90089, USA, e-mail: cch@eecs.berkeley.edu

\* Corresponding author

## Abstract

Optical-fiber-based, hollow-core waveguides (HCWs) have opened up many new applications in laser surgery, gas sensors, and non-linear optics. Chip-scale HCWs are desirable because they are compact, light-weight and can be integrated with other devices into systems-on-a-chip. However, their progress has been hindered by the lack of a low loss waveguide architecture. Here, a completely new waveguiding concept is demonstrated using two planar, parallel, silicon-on-insulator wafers with high-contrast subwavelength gratings to reflect light in-between. We report a record low optical loss of 0.37 dB/cm for a 9- $\mu\text{m}$  waveguide, mode-matched to a single mode fiber. Two-dimensional light confinement is experimentally realized without sidewalls in the HCWs, which is promising for ultrafast sensing response with nearly instantaneous flow of gases or fluids. This unique waveguide geometry establishes an entirely new scheme for low-cost chip-scale sensor arrays and lab-on-a-chip applications.

**Keywords:** hollow-core waveguide; high-contrast subwavelength grating; gas-sensing; silicon photonics.

Conventional light guiding is achieved in a geometry where a high-refractive-index core is surrounded by a low-refractive-index cladding. In the past decade, the opposite scheme – guiding light through a low-index core surrounded by high-index cladding layers has emerged as a new tool for applications. In particular, hollow-core optical waveguides/fibers are desirable for gas sensors and gas-based non-linear optics because of the increased lengths for light-matter interaction [1, 2], and for laser surgery to guide light in mid- to far-infrared wavelength regimes that lack low-absorption materials [3, 4]. Chip-scale hollow-core waveguides (HCWs) are desirable because they enable cost-effective manufacturing of on-chip systems with the potential to monolithically integrate light sources, detectors and electronics. Chip-scale HCWs have been reported using metal [5], distributed

Bragg reflectors [6, 7] and anti-resonant reflection layers [8, 9] as the guiding reflectors. However, their use is limited due to large optical losses because of insufficient reflection.

A hollow-core waveguide is best understood by the ray optics model, with an optical beam guided by zig-zag reflections from the guiding walls [6, 7, 10]. The propagation loss is strongly dependent on the reflectivity of the walls [6, 7, 10] due to the large number of reflections for a given length (the number of reflections is  $L\lambda/2d^2$ , where  $L$  is the length of the waveguide,  $d$  is the waveguide core height and  $\lambda$  is the wavelength of light used). Low losses can be obtained for HCW with core size in the tens of  $\mu\text{m}$  [7]. However, a core of this size does not lend itself to a low bending loss or efficient fiber coupling. High-contrast sub-wavelength gratings (HCGs) have been found to offer very high reflection for surface-normal incident light [11–14]. Recently, we reported numerical simulation results of a one-dimensional (1D) waveguide guided by two parallel layers of HCGs whose periodicity is parallel to the direction of propagation [10].

In this paper, we propose and experimentally demonstrate a completely new class of two-dimensional (2D) HCW where the guided wave propagates along the HCG grating bars. The transverse guiding is provided by HCG reflections, whereas the lateral confinement is achieved by varying the HCG dimensions laterally. Thus, 2D waveguiding is achieved without any physical boundaries or sidewalls, but merely with variations of HCG dimensions to create a lateral effective refractive index. Both straight and curved waveguides are demonstrated using two parallel planar wafers, each containing a single layer of HCGs. Such a 2D waveguide has never been reported before. This is also the first experimental verification of a 2D HCG HCW design using the one-dimensional  $\omega$ - $k$  diagram [15] in combination with a very new use of the effective index method [16]. The design method is simple and intuitive. The propagation loss in a straight waveguide with a 9- $\mu\text{m}$  waveguide height is measured to be 0.37 dB/cm, the lowest reported loss for an HCW with such a small core. This sidewall-less waveguide is superior in gas sensing applications compared to other HCWs. Gases or fluids can be flown into the waveguide from the side openings, instead of from the two ends of the waveguide. The cross section is thus increased by a factor of  $L/d$ , where  $L$  is the waveguide length, and  $d$  is the core height. With Fick's laws of diffusion and depending on the exact configuration, the dynamic detection speed can be increased at least by a factor of  $L^2/d^2$ , a number that is easily 8–12 orders of magnitude. The HCG HCW demonstrated here opens up a new scheme of light guiding for low-loss HCWs, allowing for an entirely new range of applications.

## 1. HCG HCW design

A high-contrast grating consists of a single layer of grating made from a high refractive-index material (e.g., silicon, or

III–V compound semiconductor) fully surrounded by a low refractive-index material (e.g., air or oxide). HCGs have been shown to be highly reflective for surface-normal incident light with demonstration of HCG-based vertical-cavity surface-emitting lasers (VCSELs) [12–14]. In addition, HCGs can be designed to reflect incident light with polarization parallel or perpendicular to the grating bars, referred to as transverse-electric (TE) and transverse-magnetic (TM) HCGs, respectively. Recently, we reported simulation results showing that the high reflection with wide bandwidth can also be designed for incident light at glancing angles [10]. In particular, we proposed a hollow-core waveguide using HCGs with grating bars perpendicular to the direction of beam propagation with low loss [10].

In this paper, we explore experimentally and theoretically a novel 2D HCG hollow-core waveguide where grating bars run along the direction of guided wave. To explain the 2D waveguiding, we should begin with a 1D slab waveguide, as shown in Figure 1A. Figure 1A shows the schematic of a basic 1D-version of HCG HCW. The HCGs are fabricated on silicon-on-insulator (SOI) wafers with the gratings formed on a silicon (Si) layer above silicon dioxide ( $\text{SiO}_2$ ). The HCW is formed by placing two HCGs in parallel, separated by an air-gap  $d$ . Wave guiding is illustrated with ray optics [10], where the optical beam is guided by zig-zag reflections from the HCG. The HCG is designed to have very high reflectivity, so that the light is well confined in the  $x$  direction. The physical intuition of why a properly designed HCG can offer a high reflectivity can be found in the Ref. [17]. In this experiment, the polarization of the electrical field is along  $y$  direction. It is easier to understand the gratings as TM-HCGs that are designed to be highly reflective. Note this notation of TM is relative to the gratings and is actually orthogonal to the typical definition for waveguide modes.

With simple ray optics [10], the propagation loss and the effective refractive index  $n_{\text{eff}}$  of the fundamental mode are calculated using the following formulae:

$$\text{Loss}[\text{dB}/m] = -10 \tan \theta / d_{\text{eff}} \cdot \log_{10} |r|^2 \quad (1)$$

$$n_{\text{eff}} = \cos \theta = k_x / k \quad (2)$$

Here  $\theta$  is the angle between the ray and the waveguide,  $k_x$  is the propagation constant,  $k$  is the wave vector of the light in free space, and  $d_{\text{eff}}$  is the effective waveguide height.  $d_{\text{eff}}$  takes into account both the physical waveguide height  $d$  and the reflection phase  $\varphi_r$ , which is approximately  $\pi$  in general. The parameter  $d_{\text{eff}}$  can be calculated by the round-trip phase condition of the fundamental mode:

$$2k_x d + 2\varphi_r = 4\pi \quad (3)$$

$$2k_x d + 2\varphi_r = 2k_x d_{\text{eff}} + 2\pi \quad (4)$$

Next, we explain the scheme to obtain lateral guiding in a 2D HCG hollow-core waveguide. For solid-core waveguides, a typical lateral guiding design employed is the effective index method [16], which uses different  $k_x$  values in the core and cladding region. Here, we also propose the same – obtaining lateral confinement ( $y$  direction) by using different HCG designs for the core and cladding region so that the effective refractive index of the core is higher than that of the cladding [18], shown in Figure 1B. This can be achieved by varying the HCG reflection phase,  $\varphi_r$ , which determines the effective index  $n_{\text{eff}}$  of the 1D-slab waveguide in Eq. (2)–(4). To ensure overall low propagation loss, both HCGs should have high reflectivities. For a fixed HCG thickness  $t_g$ , HCG designs with different periods  $\Lambda$  and grating widths  $s$  can provide remarkably large differences in  $\varphi_r$ , while maintaining a high reflectivity; this results in a variation in effective refractive index between HCG designs on a flat surface (see Supplementary information for details). Also widely known for solid core waveguides, graded-index waveguides typically exhibit lower

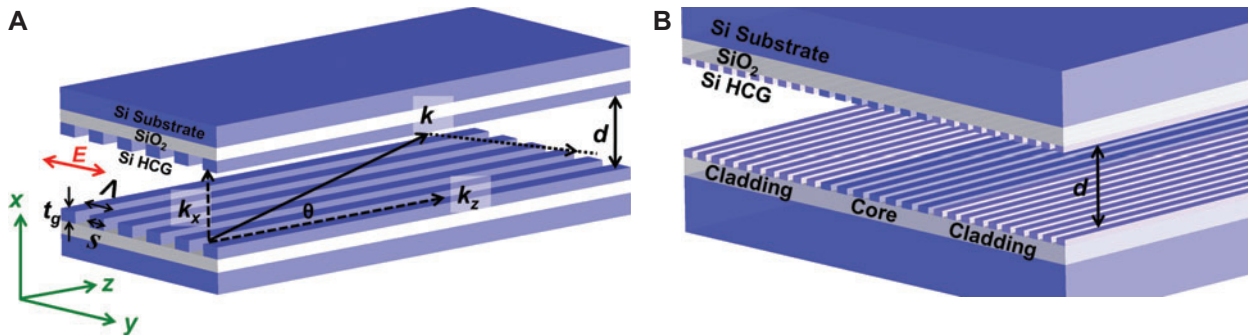


**Figure 1** The HCG HCW. (A) Schematic of a 1D slab HCG HCW. The silicon HCG sits on top of a  $\text{SiO}_2$  layer and silicon substrate. The two HCG chips are placed in parallel with a separation gap  $d$ , forming an HCW. Ray optics illustrates how light is guided: the optical beam is guided by zig-zag reflections from the HCG. The HCG is designed to have very high reflectivity, so that the light can be well confined in the  $x$  direction. The  $k$  vector is decomposed into the propagation constant  $k_x$  and transverse component  $k_z$ ;  $\theta$  is the angle between  $k$  and  $k_z$ ;  $d$  is the waveguide height;  $E$  indicates the oscillation direction of the electrical field;  $\Lambda$  is the HCG period;  $s$  is the silicon grating bar width and  $t_g$  is the HCG thickness. (B) Schematic of a 2D HCG HCW. In the lateral direction, the core and cladding are defined by different HCG parameters to provide lateral confinement.

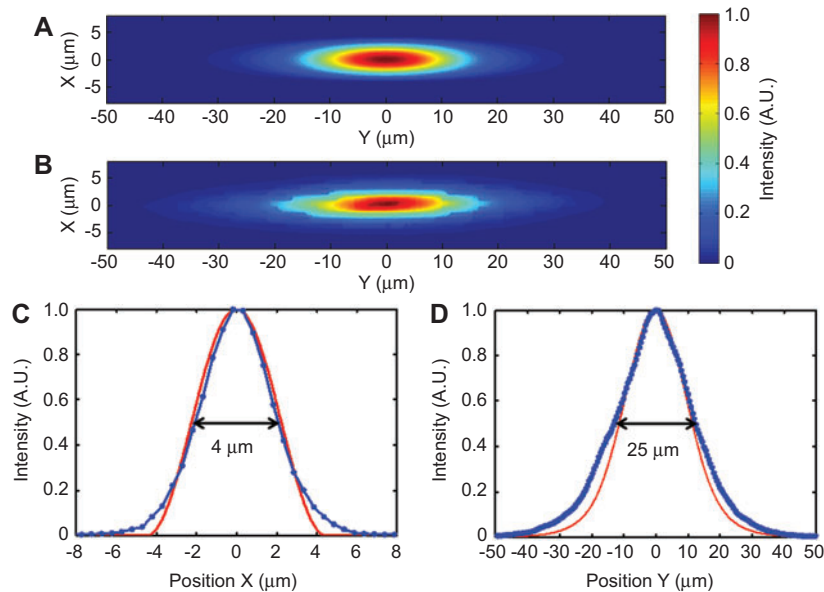


**Figure 2** Optical mode of an HCG HCW. (A) Propagation mode profile simulated by FEM. (B) The measured mode profile from the fabricated device. (C) Transverse and (D) lateral mode profile. The simulation (red curve) agrees well with experiment (blue line). The full width at half maximum (FWHM) is 4  $\mu\text{m}$  in the transverse direction, and 25  $\mu\text{m}$  in the lateral direction. The wavelength in both simulation and measurement is 1550 nm.

loss than step-index waveguides [19]. A graded effective-index profile is introduced in HCWs with chirped HCG dimensions on the order of tens of nanometers (see Supplementary information for details).

Figure 2A shows the simulated mode profile of the fundamental mode of a 2D HCG HCW. The core width  $W_c$  and the transition region width  $W_t$  are 10.9  $\mu\text{m}$  and 11.9  $\mu\text{m}$ , respectively. The cladding width of the waveguide is 42.7  $\mu\text{m}$  on each side. The resulting effective refractive index difference between the core and cladding is  $4 \times 10^{-4}$ . This waveguide configuration ensures a single lateral mode operation (see Supplementary information for details). We use rigorous coupled wave analysis [20] to calculate the complex reflection coefficient  $r$  of the HCG. Furthermore, a finite element method (FEM) is used to simulate the mode profile, resulting in an effective refractive index of 0.9961 and propagation loss of 0.35 dB/cm at 1550 nm. The minimum loss is 0.31 dB/cm at 1535 nm. It is truly remarkable to note that, although the guided mode has very little energy in the HCGs, the effective index method can be realized with a simple and small parameter change of the HCG.

## 2. Experimental results

The HCG HCW is fabricated using deep ultra-violet lithography on 6-inch SOI wafers, followed by a standard etching process (see Supplementary information for details). Using the effective index method to obtain lateral guiding, only a single etching step is required. Waveguides are cut into different lengths for loss measurement. Light is butt-coupled from

the waveguide to the photodetector (see Methods for details on the experimental setup).

Light guiding in the HCG HCW is experimentally confirmed by launching a laser beam into the waveguide and measuring the intensity profile at the output facet. Figure 2B shows the output image with the waveguide height  $d$  set to 9  $\mu\text{m}$ . The waveguide operates at fundamental mode. The measured profiles in the transverse and lateral direction are shown in Figure 2C and 2D with 4  $\mu\text{m}$  and 25  $\mu\text{m}$  full width at half maximum (FWHM), respectively, at a wavelength of 1550 nm. Excellent agreement is obtained between simulation and experiment.

The net propagation loss and coupling loss are extracted from waveguides [varying lengths, for a waveguide height of 9  $\mu\text{m}$  (see Supplementary information for details)]. Figure 3A shows the measured total loss spectrum for straight waveguides with lengths of 18 mm, 38 mm, 58 mm and 78 mm. The extracted propagation loss spectrum agrees well with the results of the simulation (Figure 3B). The minimum loss value from experiment is 0.37 dB/cm at 1535 nm, slightly higher than the simulated value. This difference is attributed to a slight warping of the two HCG chips across their length, which leads to a variation in core height on the order of  $\pm 1$   $\mu\text{m}$ . Furthermore, HCG surface roughness scattering may cause additional loss. The coupling loss is estimated to be 4 dB. This can be further reduced by improving the coupling design.

To better understand the loss of the 2D-confined propagation mode, we use FEM to simulate the loss spectra for a 1D slab HCG HCW with uniform HCG, both for the core and cladding design, shown in Figure 3B. It can be seen that the loss spectrum of the 2D-confined propagation mode follows and agrees

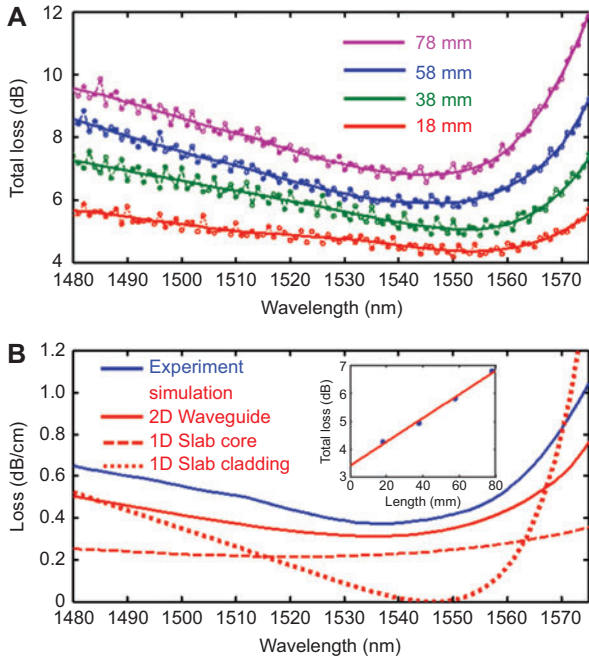


**Figure 3** Loss spectrum of the HCG HCW with a 9- $\mu\text{m}$  waveguide height. (A) Total loss spectrum for an HCG HCW with four different lengths. The dashed dot line is the measured data. The oscillation is due to the laser and a residual Fabry-Perot cavity in the optical path of the measurement system. To remove this noise, a smoothing spline method is applied. The solid curves show the smoothed spectra. (B) The experimental extracted propagation loss as a function of wavelength (blue) and the simulated loss spectrum obtained by FEM (red, solid). The simulated loss spectrum for the 1D slab HCG HCWs with pure core (red, dashed) or cladding (red, dotted) design are also shown. Inset: the linear curve fitting (red curve) to the measured data (blue dots) used to extract the propagation loss and coupling loss at 1535 nm.

well with the 1D propagation mode. With further optimization of the HCG dimensions, an even lower loss can be expected.

### 3. Control of lateral confinement

The effective index method is the main concept for the proposed lateral confinement scheme. It is further tested and illustrated by varying the waveguide height  $d$ . As seen in Figure 1A and Eq. (3–4), for a round trip in the transverse direction, the beam acquires phase through two components: interaction with the HCG (associated with a phase of  $2\varphi_c$ ) and travel through the air trajectory (associated with a phase of  $2k_x d$ ). Since  $d$  is the same for both the core and cladding regions, it is the HCG phase that creates the effective index difference (labeled as  $\Delta n/n_{\text{core}}$ ). As  $d$  is reduced, the contribution from the HCG increases relative to the air trajectory, and thus  $\Delta n/n_{\text{core}}$  becomes more pronounced. This distinction results in a stronger lateral confinement and a narrowing of the mode profile with reduced  $d$ . Figure 4A and B show the experimental measured mode profiles and the lateral FWHM vs.  $d$ , respectively. Excellent agreement is obtained with the simulated  $\Delta n/n_{\text{core}}$

value. See the video clips in the supplementary materials for intuitive illustrations of this lateral confinement.

The propagation loss, on the other hand, is not monotonically dependent on  $d$ , as shown in Figure 4C. This is because the waveguide loss consists of both transverse and lateral components. A larger  $d$  leads to a weaker lateral confinement, and thus a larger lateral loss. However, the transverse loss decreases since it is proportional to  $1/d^2$ . Thus there is an optimal  $d$  that corresponds to the lowest loss at a specific wavelength. Figure 4C shows the measured loss of the straight waveguide as a function of  $d$  at 1535 nm wavelength (see Supplementary information for details of the data processing). When  $d$  is 9  $\mu\text{m}$ , a minimum loss of 0.37 dB/cm is achieved, consistent with Figure 3. As  $d$  increases to 10  $\mu\text{m}$ , the lateral loss dominates and the overall loss increases. In general, the experimental loss agrees with the simulated loss. For a larger core height, the discrepancy is more pronounced, a consequence attributed to the coupling into higher order modes.

To further illustrate lateral index guiding, we fabricated various waveguides on the same chip with uniform HCG design (with the core and cladding sharing the same HCG design) and anti-guiding design (with the core and cladding designs swapped from the original configuration). The output mode profiles are presented in Figure 4D, and they show distinct differences with light dispersed in the waveguide without the appropriate HCG design. These lateral confinement measurements demonstrate the effectiveness of the effective index method for an HCW for the first time. It is truly remarkable that with little optical energy in the HCG, lateral guiding can be obtained with a planar structure. This enables light to be guided in an HCW without the aid of physical side reflectors, and opens up a new regime of optical waveguiding.

### 4. Light guiding in curved HCG HCWs

Light can also stay guided around curves by this side-wall-less waveguides. Figure 5A shows a top view of the “S-shape” and “double-S-shape” curved waveguide layout. The “S-shape” waveguide demonstrates light guiding by the bend with light launched at port A and light output observed at port A’ rather than B’. At the bending section, the mode profile is similar to that of a straight waveguide but with its center shifted towards the waveguide edge that is farther from the center of the curving radius. This is the same case as a solid-core curved waveguide [21] with the conventional index guiding mechanism. The “double-S-shape” waveguide is used to extract the bending loss, with various waveguide length combinations. Figure 5B shows the loss spectra for various bending radii  $R$  extracted from the 18 mm to 38 mm long waveguides, with a waveguide height  $d$  of 6  $\mu\text{m}$ . It is seen that as the bending radius of curvature decreases, the loss spectrum slightly red-shifts. This is because lateral confinement tends to be stronger at longer wavelengths, as indicated by the FEM simulated spectrum of  $\Delta n/n_{\text{core}}$  shown in Figure 5C. This also explains why the loss difference between the straight and the curved waveguides

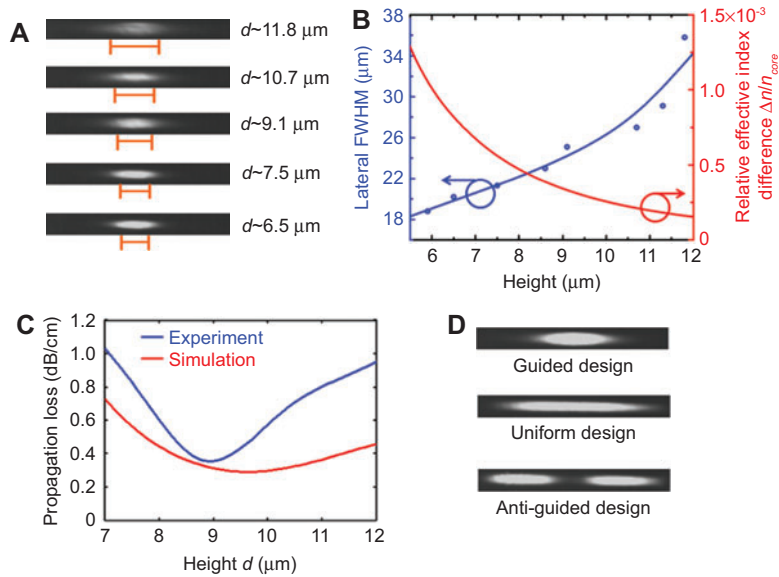


**Figure 4** Lateral confinement in the HCG HCW. (A) Mode profile at different waveguide heights  $d$ . As  $d$  decreases,  $n/n_{\text{core}}$  increases, and the mode is more confined with reduced lateral leakage. The guidelines indicate the FWHM of the mode in the lateral direction. (B) Experimental lateral FWHM of the fundamental mode vs. waveguide height  $d$  (blue dots as experiment sampling points, curve-fitted with blue curve). The  $\Delta n/n_{\text{core}}$  value of the fundamental mode simulated by FEM is shown in red. The wavelength for the measurement is 1550 nm. (C) Propagation loss vs. waveguide height  $d$  at a wavelength of 1535 nm. At the optimized waveguide height of 9  $\mu\text{m}$ , an optimal tradeoff between lateral leakage and transverse leakage is achieved. The FEM simulated loss for the fundamental mode is also plotted, in reasonable agreement with experiment. (D) Mode profiles for three side-by-side HCWs ( $d$  being constant at  $\sim 9$   $\mu\text{m}$ ), with lateral guiding (top), uniform design (middle) where the core and cladding share the same HCG design and anti-guided design (bottom) where the core and cladding designs are swapped from the guiding design. For the mode profiles in (A) and (D), the output power of the mode is kept constant respectively. The image window is 140  $\mu\text{m}$  by 16  $\mu\text{m}$ . The wavelength is set to 1550 nm.

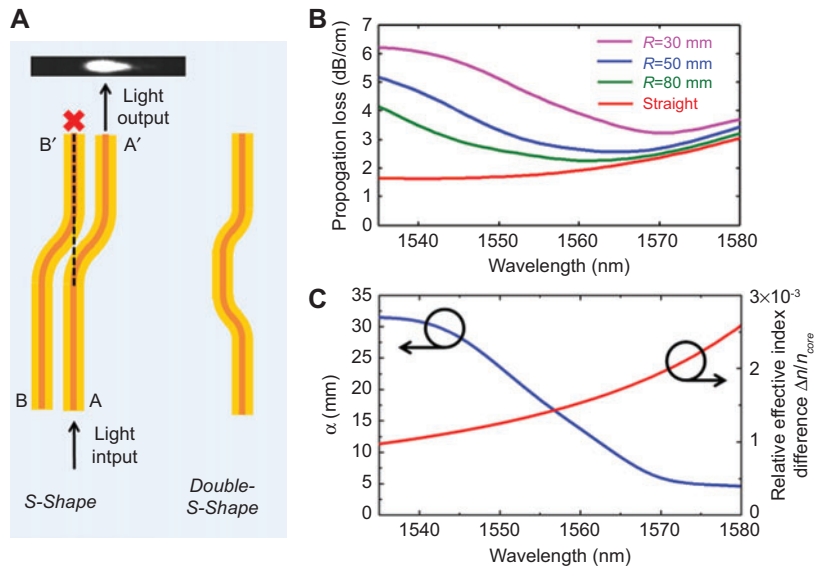


**Figure 5** A curved HCG HCW. (A) Layout of the ‘‘S-shape’’ and ‘‘double-S-shape’’ curved waveguides. For the ‘‘S-shape’’ layout, curved waveguides A-A’ and B-B’ are parallel, and the input port of A-A’ is aligned with the output port of B-B’. Light is launched into port A. Light guiding by the bend is demonstrated with the output observed in A’ rather than B’. (B) Experimental loss spectrum for waveguides with different radii of curvature  $R$ , extracted from various waveguide length combinations of the ‘‘double-S-shape’’ curved waveguide layout. The loss includes both the propagation loss and the mode coupling loss at the four bending junctures for an 18-mm long waveguide. (C) The slope of the linear fit of loss vs.  $R^{-1}$ ,  $\alpha$ , as a function of wavelength; this is consistent with the FEM simulated  $\Delta n/n_{\text{core}}$  spectrum. See Supplementary information for more details.

becomes smaller as the wavelength increases. To quantify this, a linear fit is applied to the loss as a function of  $R^{-1}$  for each wavelength, and the slope  $\alpha$  is extracted (see Supplementary information for a detailed expression of  $\alpha$ ), as plotted in Figure 5C. The slope of this graph indicates how well the light is confined to the waveguide. The slope decreases with increasing wavelength, consistent with the simulated spectrum of  $\Delta n/n_{\text{core}}$ .

## 5. Discussion

The demonstration of lateral confinement in planar HCG HCWs opens up a new scheme of waveguide engineering through surface phase manipulation. Keeping the HCG thickness fixed, different periods and grating bar widths are able to provide different reflection phases, while maintaining a high reflectance. This sidewall-free HCW design is a strong candidate for use in compact, low-power, fast on-chip gas/fluid sensor arrays and lab-on-a-chip applications. With no sidewall, gaseous or fluidic molecules can penetrate into the waveguide instantaneously compared to a conventional HCW, where only the input and output ends serve as inlet and outlet for the gas. We estimate the speed increase to be 8~12 orders of magnitude (see Supplementary information for details). Dispersion can also be engineered based on the reflection phase spectrum, and hence, slow light and fast light waveguides can be engineered. Other potential applications of this waveguide scheme include radio-frequency (RF) filters and low noise oscillators, optical routers and couplers based on multi-mode interference, etc.

The planar structure of the waveguide makes fabrication simple. The HCG thickness is kept constant, and thus only one step of etching is required. While the waveguides presented in this paper are formed from two pieces of HCG chips and offer a proof-of-concept, monolithic integration is possible by flip-chip bonding or by processing on a multi-stack silicon oxide wafer.

In summary, we present the first experimental device showing lateral confinement in a low-loss planar HCW structure. The effective index method is demonstrated for the first time in a planar waveguide structure, as well as in an HCW. The measured propagation loss is the lowest among all HCWs that are mode-matched to a single-mode optical fiber. Further optimization of the HCG dimensions based on the loss contour and effective index contour map (see Figure S1 in Supplementary information) can lower the loss to  $<0.1$  dB/cm for a straight waveguide in FEM simulations. This is a result of the high reflectivity of the HCG, as well as the unique lateral confinement scheme. Radius of curvature and loss of the curved waveguide can also be reduced by further optimization of the effective index. As an example, we design  $\Delta n/n_{\text{core}} \sim 2.1 \times 10^{-3}$  for a 5- $\mu\text{m}$  height waveguide. The straight waveguide loss is 0.442 dB/cm, whereas the bending loss is 1.026 dB/cm and 8.839 dB/cm for a radius of curvature  $R=15$  mm and 10 mm respectively in FEM simulation. Further optimization of the waveguide

configuration is possible to reduce  $R$  to below 10 mm while maintaining a low loss. The unique waveguide structure presented here establishes a new regime of waveguiding in HCWs.

## 6. Methods

**Optical mode imaging and loss measurement.** To characterize the light guiding in the HCG HCW, a laser beam from a tunable laser source (Agilent 81680A) is first polarization adjusted and then collimated by a fiber collimator, and launched into the HCG HCW sample by a 10X (N.A.=0.25) objective. The Gaussian beam waist size at the waveguide's input facet is optimized such that only the fundamental mode is excited. A 50X (N.A.=0.5) objective is used to collect the light for output facet imaging. With precise alignment of the two chips, an optical mode can be seen at the output facet.

For loss measurement, the laser is internally modulated at 1 kHz. The 50X objective is replaced with a photodetector that butt-couples the light from the waveguide in order to allow the optical power to be measured with a lock-in amplifier (Stanford Research Systems SR850). Alternatively, the 50X objective can be used to collect the light. The light is then spatially filtered by a pinhole and focused onto a photodetector. These two light detection methods are equivalent when the waveguide height  $d$  is small and lateral light leakage is negligible. However, as  $d$  increases such that lateral leakage becomes substantial, the spatial filter ensures that only the light in the waveguide is detected, which is essential for measuring the loss as a function of  $d$ .

## Acknowledgements

The authors acknowledge Professors Eli Yablonovitch, Fumio Koyama, Markus Amann, Shun-Lien Chuang and Xiaoxu Deng, Drs. Forrest Sedgwick and Vadim Karagodsky for fruitful discussions. This work was supported by DARPA iPHOD HR0011-09-C-0124. C.C.H. thanks support of DoD National Security Science and Engineering Faculty Fellowship, Chang Jiang Scholar Endowed Chair Professorship and Humboldt Research Award.

## Author contributions

C.C.H. proposed and guided the overall project. W.Y., C. C., M.C.W., and C.C.H. designed the experiments. W.Y., J.F., Y.Y., A.E.W. and C.C.H. designed the HCG HCW structure and performed simulation. W.Y., J.F. and K.G. fabricated the device. W.Y. and A.Y. performed optical characterization on the device. W.Y. and C.C.H. composed the manuscript.

## Additional information

The authors declare no competing financial interests. Supplementary information accompanies this paper at <http://www.degruyter.com/view/j/nanoph>. Reprints and permission information is available online at <http://www.degruyter.com/view/j/nanoph>. Correspondence and requests for materials should be addressed to C.C.H.

## References

- [1] Saito Y, Kanaya T, Nomura A, Kano T. Experimental trial of a hollow-core waveguide used as an absorption cell for concentration measurement of  $\text{NH}_3$  gas with a  $\text{CO}_2$  laser. *Opt Lett* 1993;18(24):2150–2.
- [2] Benabid F, Knight JC, Antonopoulos G, Russell P, St J. Stimulated Raman scattering in hydrogen-filled hollow-core photonic crystal fiber. *Science* 2002;298(5592):399–402.
- [3] Temelkuran B, Hart SD, Benoit G, Joannopoulos JD, Fink Y. Wavelength-scalable hollow optical fibres with large photonic bandgaps for  $\text{CO}_2$  laser transmission. *Nature* 2002;420:650–3.
- [4] Shurgalin M, Anastassiou C. A new modality for minimally invasive  $\text{CO}_2$  laser surgery: flexible hollow-core photonic band-gap fibers. *Biomed Instrum Technol* 2008;42(4):318–25.
- [5] Bicknell R, King L, Otis CE, Yeo J-S, Meyer N, Kornilovitch P, Lerner S, Seals L. Fabrication and characterization of hollow metal waveguides for optical interconnect applications. *Appl Phys A* 2009;95(4):1059–66.
- [6] Miura T, Koyama F, Matsutani A. Modeling and fabrication of hollow optical waveguide for photonic integrated circuits. *Jpn J Appl Phys* 2002;41(1,7B):4785–9.
- [7] Miura T, Koyama F. Low-loss and polarization-insensitive semiconductor hollow waveguide with GaAs/AlAs multi-layer mirrors. *Jpn J Appl Phys* 2004;43(1A/B):L21–3.
- [8] Yin D, Schmidt H, Barber JP, Hawkins AR. Integrated ARROW waveguides with hollow cores. *Opt Express* 2004;12(12):2710–5.
- [9] Yang W, Conkey DB, Wu B, Yin D, Hawkins AR, Schmidt H. Atomic spectroscopy on a chip. *Nature Photon* 2007;1:331–5.
- [10] Zhou Y, Karagodsky V, Pesala B, Sedgwick FG, Chang-Hasnain CJ. A novel ultra-low loss hollow-core waveguide using subwavelength high-contrast gratings. *Opt Express* 2009;17(3):1508–17.
- [11] Mateus CFR, Huang MCY, Chen L, Chang-Hasnain CJ, Suzuki Y. Broad-band mirror (1.12–1.62  $\mu\text{m}$ ) using a subwavelength grating. *IEEE Photon Technol Lett* 2004;16(7):1676–8.
- [12] Huang MCY, Zhou Y, Chang-Hasnain CJ. A surface-emitting laser incorporating a high-index-contrast subwavelength grating. *Nature Photon* 2007;1:119–22.
- [13] Chang-Hasnain CJ, Zhou Y, Huang MCY, Chase C. High-contrast grating VCSELs. *IEEE J Sel Topics Quantum Electron* 2009;15(3):869–78.
- [14] Chase C, Rao Y, Hofmann W, Chang-Hasnain CJ. 1550 nm high contrast grating VCSEL. *Opt Express* 2010;18(15):15461–6.
- [15] Karagodsky V, Pesala B, Sedgwick FG, Chang-Hasnain CJ. Dispersion properties of high-contrast grating hollow-core waveguides. *Opt Lett* 2010;35(24):4099–101.
- [16] Knox RM, Toullos PP. Integrated circuits for the millimeter through optical frequency range. Fox J ed. Polytechnic Press, Brooklyn. *Proc MRI Symp Submillimeter Waves* 1970;497–516.
- [17] Karagodsky V, Sedgwick FG, Chang-Hasnain CJ. Theoretical analysis of subwavelength high contrast grating reflectors. *Opt Express* 2010;18(16):16973–88.
- [18] Pesala B, Karagodsky V, Koyama F, Chang-Hasnain CJ. Novel 2D high-contrast grating hollow-core waveguide. Optical Society of America. *Conf on Lasers and Electro-Optics/ Int Quant Electron Conference*, 2009.
- [19] Hu J, Feng N-N, Carlie N, Petit L, Wang J, Agarwal A, Richardson K, Kimerling L. Low-loss high-index-contrast planar waveguides with graded-index cladding layers. *Opt Express* 2007;15(22):14566–72.
- [20] Moharam MG, Gaylord TK. Rigorous coupled-wave analysis of planar-grating diffraction. *J Opt Soc Am* 1981;71(7):811–8.
- [21] Marcatili EAJ. Bends in optical dielectric guides. *Bell Syst Tech J* 1969;48(7):2103–32.

Received February 3, 2012; accepted May 22, 2012